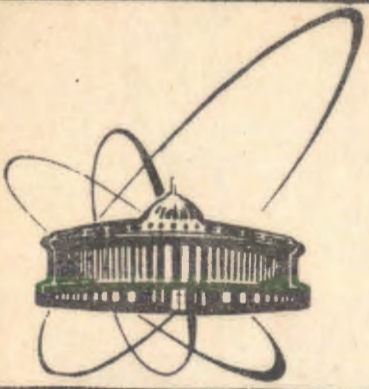

объединенный
институт
ядерных
исследований
дубна

E3-91-428

M.A. Ali, A.A.Bogdzel, V.A.Khitrov, Yu.V.Kholnov,
V.D.Kulik, L.H.Khiem, N.T.Tuan, P.D.Khang,
Yu.P.Popov, V.N.Shilin, A.M.Sukhovoj,
E.V.Vasilieva, A.B.Vojnov

INTENSE TWO-STEP CASCADES OF ^{158}Gd COMPOUND-STATE DECAY

Submitted to "Nuclear Physics A"

1991

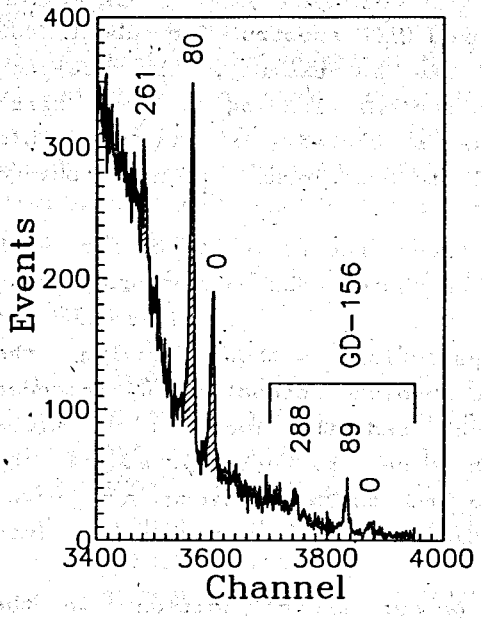

Fig.1. A part of summed coincidences spectrum for ^{158}Gd. Shaded areas correspond to the useful events. Figures over peaks denote the energies (in keV) of finel cascade levels.

The time resolution of the two Ge(Li) detectors used in the experiment was about (10 to 12) ns for a ^{60}Co γ-ray source. The time window for selected coincidences was =40 ns. The germanium detectors had efficiencies of about 5% and 10% relative to a NaI crystal having a 76 mm diameter and 76 mm thickness. Lead filters of 2.5 g.cm^{-2} are interposed between the germanium detectors to minimize their detection of the backscattered γ-quanta[5]. The energy resolution of these detectors was about 3.5 keV at 1332 keV. All other experimental and technical details are given in ref.[5]. With this arrangement we had a total efficiency of 2x10^{-5} events per decay for the 2505 keV sum peak energy of ^{60}Co.

3. Results and discussion

Because of the small partial widths of these cascades and the small efficiency of the Ge(Li) detectors employed, the acquisition of SACP spectra with reasonable statistical precision is necessary if any meaningful measurements are to

be made. A part of the measured SACP spectrum for about 400 hours is displayed in fig.1. As an example, the measured intensity distribution for a cascade leading to the first excited state in ^{158}Gd is presented in fig.2. This distribution corresponds only to coincidences from the shaded peaks in fig.1.

The main peculiarity of these spectra is that for each cascade there exists a pair of photo-peaks having equal areas and widths; if the approach of the numerical method to improve the amplitude resolution without losing the efficiency[1]) is applied. The absolute intensities of cascades are proportional to peak areas and the location of these transitions in the decay scheme can be established if the cascade energies (determined from peaks positions) are known.

The intensity distribution is usually decomposed into two components :

1- Some dozens of intense peaks; their positions in the spectra determine the cascade transition energies. The mean energy error, in our data, was $\langle\sigma\rangle$ = 1.55 keV. The intensity of a given cascade $i_{\gamma\gamma}$ is defined as the ratio between its area and the total spectrum area. In other words, it is related to the total sum over all possible (including unresolved) cascades which have the same total energy.

2- A continuous distribution arising from a large number of low-intensity cascades. According to our experience, this part may have, in itself, about (30 to 40)% of the total area of the spectrum.

Intense, and well resolved, cascades afford much help[7]) in the construction of the decay schemes for complex nuclei up to an excitation energy of 3-4 MeV. It is well established that the information about the final levels, to which the cascades decay with two given transitions, considerably increases our confidence in the predicted decay scheme[2]). The probability of a false level with an energy below 3 MeV to appear in the decay scheme does not exceed 10% , if the decay scheme is compiled by the algorithm given in ref.[7]).

Table 1.

A list of the energies, E_1 and E_2, of the cascades transitions and their relative intensities $i_{\gamma\gamma}\pm\Delta i_{\gamma\gamma}$ in percent of the total intensity of the two-step cascades which have the same total energy. $E_M\pm\Delta E_M$ is the intermediate levels energy excited by the primary transition

N	E_1,keV	E_2,keV	$i_{\gamma\gamma}(\Delta i_{\gamma\gamma})$	$E_M(\Delta E_M)$,keV
	$E_1 + E_2$ = 7937.4 keV		(E_f = 0 keV)	
1	6980.9	956.6	0.33(0.12)	
2	6870.6	1066.9	0.55(0.13)	
3	6777.0	1160.4*)	1.74(0.47)	
4	6750.3	1187.2	24.62(1.01)	1187.2(6)
5	6428.4	1509.1	0.91(0.25)	
6	6420.3	1517.2	3.15(0.30)	1517.2(6)
7	6250.9	1686.5*)	0.57(0.20)	
8	6178.5	1758.9	0.52(0.20)	
9	5972.5	1965.0	2.68(0.30)	(1965.0)
10	5879.8	2058.0	0.39(0.35)	
11	5807.5	2129.8	0.81(0.30)	(2130.0)
12	5725.0	2212.4	0.75(0.28)	2214.0(19)
13	5678.0	2259.4	2.18(0.38)	2260.0(8)
14	5670.7	2267.8	0.36(0.36)	
15	5577.5	2359.9	0.98(0.39)	(2360.0)
16	5320.3	2617.2	0.63(0.36)	
17	5280.7	2656.8	1.16(0.37)	2656.9(10)
18	5263.7	2673.6	0.63(0.36)	
19	5135.2	2802.2	1.45(0.32)	(2802.0)
20	5108.8	2828.6	0.63(0.30)	2829.9(11)
21	5092.7	2844.7	0.71(0.31)	
22	5082.9	2854.5	0.99(0.31)	2854.7(9)
23	5059.4	2878.1	0.54(0.30)	2878.8(8)
24	4999.7	2934.4	0.93(0.37)	
25	4975.6	2961.9	1.03(0.36)	(2962.0)
26	2969.7	4967.8	0.54(0.40)	4968.1(23)
27	4872.7	3064.7	0.58(0.33)	3063.7(19)
28	4840.6	3096.6	0.72(0.36)	
29	3106.3	4831.1	1.40(0.40)	4830.9(9)

N	E_1,keV	E_2,keV	$i_{\gamma\gamma}(\Delta i_{\gamma\gamma})$	$E_M(\Delta E_M)$,keV
30	4654.8	3281.4	0.42(0.20)	
31	4646.1	3291.6	1.03(0.32)	(3292.0)
32	4481.3	3456.1	0.60(0.31)	
33	4430.8	3506.6	1.00(0.33)	
34	4412.0	3525.5	1.00(0.34)	
35	4367.4	3570.1	0.92(0.35)	3570.9(12)
36	4336.9	3600.6	1.08(0.36)	3600.5(10)
37	4324.5	3613.0	1.08(0.37)	
38	4278.6	3658.9	0.89(0.36)	3659.5(11)
39	4193.9	3743.5	1.01(0.36)	
40	4084.8	3852.9	0.96(0.38)	
41	4012.8	3924.7	0.80(0.30)	3923.3(11)
42	3987.2	3950.4	0.82(0.32)	

$E_1 + E_2 =$ 7857.9 keV (E_f = 79 keV)

1	6913.2	944.6	2.30(0.17)	(1024.0)
2	6750.2	1107.6	13.55(0.48)	1187.2(6)
3	6695.4	1162.5	0.28(0.13)	
4	6672.3	1185.6	1.95(0.17)	(1265.0)
5	6419.9	1438.0	1.23(0.14)	1517.2(6)
6	6147.7	1710.1	0.37(0.13)	(1790.0)
7	5981.8	1876.0	0.28(0.16)	(1955.0)
8	5956.0	1901.9	0.35(0.16)	
9	5903.1	1954.8	0.51(0.16)	(2034.0)
10	5785.1	2072.7	0.48(0.16)	(2152.0)
11	5723.2	2134.6	0.42(0.17)	2214.0(19)
12	5676.8	2181.0	2.34(0.29)	2260.0(8)
13	5662.4	2195.4	1.75(0.28)	2276.3(13)
14	5653.5	2204.4	1.01(0.25)	(2283.0)
15	5615.6	2242.2	0.57(0.22)	2322.2(10)
16	5591.6	2266.4	0.62(0.22)	(2346.0)
17	5571.7	2285.5	0.58(0.22)	
18	5543.8	2314.4	1.09(0.24)	(2394.0)
19	5437.3	2420.6	0.75(0.19)	(2500.0)
20	5398.5	2459.3	0.53(0.19)	(2539.0)
21	5342.9	2514.9	0.74(0.21)	(2595.0)
22	5335.7	2522.2	0.70(0.21)	(2602.0)

N	E_1,keV	E_2,keV	$i_{\gamma\gamma}(\Delta i_{\gamma\gamma})$	$E_M(\Delta E_M)$,keV
23	5311.2	2546.6	0.24(0.19)	
24	5280.1	2577.7	0.42(0.20)	2656.9(10)
25	5239.7	2618.1	0.57(0.23)	(2697.0)
26	5186.9	2670.9	0.81(0.24)	(2750.0)
27	5177.8	2680.0	2.61(0.29)	(2760.0)
28	5154.4	2703.5	0.75(0.24)	(2783.0)
29	5106.7	2751.2	0.67(0.22)	2829.9(11)
30	5082.4	2775.5	0.55(0.22)	2854.7(9)
31	5068.3	2792.4	0.21(0.14)	
32	5058.0	2799.8	1.44(0.29)	2878.8(8)
33	4967.1	2890.7	0.33(0.28)	
34	4939.3	2918.5	0.76(0.27)	(2999.0)
35	4928.6	2929.2	1.48(0.29)	3008.3(9)
36	2938.3	4919.6	0.38(0.27)	4997.7(11)
37	4908.0	2950.2	0.74(0.27)	(3030.0)
38	4875.1	2982.8	1.00(0.27)	3063.7(19)
39	4843.4	3014.8	0.98(0.25)	
40	4819.8	3037.3	0.54(0.25)	
41	4809.9	3047.5	0.77(0.24)	(3127)
42	4795.9	3062.0	0.79(0.25)	(3141)
43	4784.5	3072.7	0.74(0.25)	(3152)
44	4766.3	3090.8	0.64(0.25)	
45	3107.0	4750.9	0.52(0.27)	4830.9(9)
46	4738.8	3119.1	1.47(0.28)	
47	4687.0	3170.9	0.60(0.24)	
48	4678.0	3179.9	0.27(0.23)	
49	4666.5	3191.3	0.30(0.22)	
50	4623.2	3234.4	0.44(0.21)	
51	4595.0	3262.9	0.68(0.23)	
52	4552.4	3305.4	0.60(0.23)	
53	4534.0	3323.9	0.47(0.23)	
54	4502.6	3355.6	0.78(0.22)	
55	4490.9	3366.7	0.54(0.22)	
56	4365.1	3492.7	0.45(0.21)	3570.9(12)
57	4336.8	3521.0	0.51(0.22)	3600.5(10)
58	4304.0	3553.6	0.28(0.18)	
59	4277.3	3580.6	0.47(0.20)	3659.5(11)

N	E_1,keV	E_2,keV	$i_{\gamma\gamma}(\Delta i_{\gamma\gamma})$	$E_M(\Delta E_M)$,keV
60	4261.0	3596.9	0.59(0.19)	
61	4234.2	3623.7	0.52(0.19)	3702.6(12)
62	4218.6	3636.8	0.28(0.18)	
63	4204.0	3653.7	0.46(0.19)	
64	4188.7	3669.1	0.49(0.20)	
65	4075.5	3782.4	0.4190.22)	
66	4060.4	3797.4	0.54(0.22)	
67	4041.0	3816.8	0.43(0.22)	
68	4023.6	3837.5	0.44(0.34)	
69	4014.9	3842.9	0.79(0.34)	3923.3(11)
70	3955.2	3902.6	0.54(0.22)	
	$E_1 + E_2$ = 7676.0 keV		(E_f = 261 keV)	
1	6757.9	918.2	3.69(0.79)	(1179.0)
2	6750.0	925.9	5.55(0.89)	1187.2(6)
3	6488.8	1187.1	2.56(0.41)	(1454.0)
4	6420.4	1255.6	1.98(0.46)	1517.2(6)
5	5927.1	1748.9	0.94(0.43)	
6	5821.5	1854.4	1.05(0.63)	
7	5720.5	1955.5	1.06(0.60)	2214.0(19)
8	5659.8	2016.2	3.34(0.66)	2276.3(13)
9	5614.7	2061.3	1.48(0.63)	2322.2(10)
10	5418.0	2258.0	1.99(0.85)	
11	5292.9	2383.1	1.67(0.79)	(2644.0)
12	5258.4	2417.6	1.45(0.79)	
13	5235.6	2440.2	2.72(0.85)	(2702.0)
14	5129.4	2546.6	2.19(0.95)	
15	5059.4	2616.6	2.10(0.89)	2878.8(8)
16	4993.5	2682.5	2.97(0.99)	
17	4930.0	2746.0	2.25(0.99)	3008.3(9)
18	4870.9	2805.1	2.13(1.01)	3063.7(19)
19	2939.9	4736.1	3.46(1.08)	4997.7(11)
20	2968.8	4707.2	1.08(1.01)	4968.1(23)
21	4499.7	3176.2	1.60(0.97)	
22	4340.9	3335.1	1.80(1.10)	
23	4236.2	3439.8	1.77(1.07)	3702.6(12)
24	4126.4	3549.7	2.21(0.76)	

N	E_1,keV	E_2,keV	$i_{\gamma\gamma}(\Delta i_{\gamma\gamma})$	$E_M(\Delta E_M)$,keV
25	4118.7	3557.5	1.93(0.80)	
26	4069.8	3606.2	2.33(1.03)	

Notes.

(*) denotes the first escape peak of the primary transition of the cascades 8536 → E_M → 89 keV in ^{156}Gd. These peaks represent the more intense peaks of the background which appears in our measurements.

Table 2

Total experimental, $I^E_{\gamma\gamma}$, and calculated, $I^T_{\gamma\gamma}$, intensities (in % per decay) of cascades leading to the three low-lying levels, E_f, in ^{158}Gd

E_f keV	$I^E_{\gamma\gamma}$	Calculation of the level density models: [10]	[11]	[10]a)	[11]a)
0	4.6(2)	1.7	2.4	1.5	2.6
79	11.3(4)	5.6	8.2	5.1	8.1
261	3.2(2)	1.7	2.8	1.5	2.6
Sum:	19.1	9.0	13.4	8.1	13.3

a) is put for the predicted values from the developed model of radiative strength function reported in ref.[13]).

Table 1 lists all the intense cascades (shown in fig.2) and observed as pairs of resolved peaks. The algorithm[7]) allows us to locate these cascades in the decay scheme, independently of Ritz's rule. Much more information could be obtained if the cascade intensity distribution is analysed in terms of its primary transition energy, or analysed as a function of the excitation energy of the intermediate level. Thus, each spectrum (in fig.2) must be decomposed into components related to primary or secondary transitions. A method of such analyses is described in ref.[8]). Such decomposition is made here by using the data listed in table 1. If the proposed intermediate level of a cascade, E_M, has been put in brackets in table 1, then the quanta sequence in cascades has been taken from literature[9]) and not from the analysis by algorithm [7]) . If the value E_M is not given, this means that the cascade cannot be placed in the decay scheme by using the algorithm[7]). Such cascades are considered[8]) and analysed by assuming that the soft quanta comes from a primary transition.

The total intensity $I_{\gamma\gamma} = \Sigma A_{\gamma\gamma}$, where $A_{\gamma\gamma} = (i_1 i_2 / \Sigma i_2)$, of all the cascades (including unresolved ones) is determined from the data listed in table 1 and ref.[9]), using the absolute intensity i_1 of the primary transitions with E_1= 6750 keV (i_1=2.8 % per decay) and E_1= 6420 keV (i_1=0.36 % per decay). The branching coefficients ($i_2 / \Sigma i_2$) are determined from the spectrum of soft γ-quanta in coincidence with these transitions. From these coefficients, we have calculated the intensities, $I^E_{\gamma\gamma}$, for all the two-step cascades leading to the final three low-lying states in ^{158}Gd. The energy of the intermediate level lies in the energy interval (B_n - 0.52) $\geq E_M \geq$ (E_f+0.52). This threshold energy (0.52 MeV) was chosen[5]) to minimize the experimental systematic-errors. Table 2 shows a comparison between the experimental, $I^E_{\gamma\gamma}$, and theoretical, $I^T_{\gamma\gamma}$, values as calculated using the models of refs.[10,11]).

4. Decay scheme of ^{158}Gd

The decay scheme of the ^{158}Gd compound state, listed in table 1 by applying the algorithm[7]), is, in general, in good agreement with most of the earlier published data. However, it shows some remarkable difference from that reported recentely in ref.[9]). It must be noted here that table 1 lists only the cascades which have an absolute intensity $i_{\gamma\gamma} \geq 0.03$ % per decay and lead to the first three states of the rotational band $K^\pi = 0^+$ based on the ground state. The other cascades, such as those having low-intensity primary transitions or those leading to higher excited states, are beyond the scope of this study.

In this respect, we confirm the existence of the transition whose energy is 1185 keV and belongs to the decay of the intermediate level at 1265 keV. We determined an absolute intensity of 0.22% per decay for this cascade. On the other hand, no information is available concerning the secondary transition whose energy E_γ= 1004 keV and intensity $i_{\gamma\gamma}$= 0.06% per decay although this intensity[9]) is twice as much as the limit of our spectrometer sensitivity.

Moreover, we have observed the cascade transitions E_1= 6489 keV and E_2=1187 keV (leading to the level at 261 keV) with an absolute intensity $i_{\gamma\gamma}$= 0.082% per decay. This cascade was not reported in ref.[9]). The possible intermediate level of this cascade is E_M= 1454 keV; which is close to the known level[9]) at 1452 keV with $J^\pi = 0^+$. The level, at 1452 keV, cannot be considered as the intermediate level of the discussed cascade, because transitions between states with spins $2^- \rightarrow 0^+ \rightarrow 4^+$ may not have so high an intensity. Thus, we may propose the existence of another new level at 1454 keV with a possible spin value of J = 2 or 3 and unknown parity.

Also, we report here on the new two-step cascade whose primary transition energy is 5972 keV and intensity $i_{\gamma\gamma}$= 0.12% per decay and which excites the intermediate level at 1965 keV. Another group of intense cascades leading to the

three low-lying states ($E_f \leq 261$ keV) of the 0^+ rotational band based on the ground state are not found among the published data, and presumably are reported here (table 1) for the first time.

Some cascades (which mainly have soft transitions with $E_\gamma \leq 2$ MeV) cannot be placed in the well established decay scheme. This problem was discussed in ref.[3]) and it was suggested there that these soft γ- quanta are, most probably, primary transitions. A list of possible soft primary cascade transitions leading to the first three low-lying levels and the mean calculated values of the cascades intensity are given in table 3.

The data concerning weak cascades must be considered as the upper experimental estimates of the possible enhancement of soft primary transitions, since their errors $\Delta i_{\gamma\gamma} \simeq$ (30 to 50) %. The problem of intensifying the primary and secondary transitions in nuclei of the 4s-neutron resonance strength function region has been discussed earlier[4]). It was shown, in these nuclei, that there are "distinct" channeles for intense transitions, whose intensities exceed the fluctuations predicted by the statistical theory. The experimental intensities, if compared with the calculated ones, show[5]) a non-random character for the nuclei ^{165}Dy and ^{168}Er. The data listed in table 3 give the upper limit for these enhancements in ^{158}Gd.

A comparison between the experimental and calculated cascade intensities for the given primary transiton energies is demonstrated in fig.3. The cascades which are not placed in the decay scheme, and whose E_M values are not listed in table 1, are also shown in this figure by assuming that the primary cascade transitions are the hard quanta. For this case, the divergence between the experimental and the calculated intensities is minimum.

The calculated cascade intensity dependence is obtained by assuming that the level density below the neutron binding energy is described by the Fermi-gas[10]) model with

Table 3.

The experimental, $i^E_{\gamma\gamma}$, and the calculated, $i^T_{\gamma\gamma}$, average cascade intensities of some possible primary transitions E_1 and their ratios $r = (i^E_{\gamma\gamma} / i^T_{\gamma\gamma})$. E_f is the energy of the final level to which the cascade decays. The intensities are given in percentage of the total intensity summed over all the two-step cascades leading to the given final state level

E_1 keV	E_f keV	$i^E_{\gamma\gamma}$	$i^T_{\gamma\gamma}$	r	E_γ [9])	i_γ [9])
956	0	0.33(12)	$0.17*10^{-4}$	$2*10^4$	956.04	0.14
1067	0	0.55(13)	$0.25*10^{-4}$	$2*10^4$	1068.74[a]	0.015
1162	79	0.28(13)	$0.13*10^{-4}$	$2*10^4$	1161.24[a]	0.046
1509	0	0.91(25)	$0.12*10^{-3}$	$8*10^3$	1509.5[a]	0.14
1759	0	0.52(20)	$0.25*10^{-3}$	$2*10^3$	1759.2[a]	0.06
1749	261	0.94(43)	$0.25*10^{-3}$	$4*10^3$	----	--
1854	261	1.05(63)	$0.33*10^{-3}$	$3*10^3$	1857.0	0.53
1902	79	0.35(16)	$0.13*10^{-3}$	$3*10^3$	1902.9[a]	0.09

Notes

The absolute quantities of $i^E_{\gamma\gamma}$ and $i^T_{\gamma\gamma}$ can be obtained from their multiplication by $0.01*I_{\gamma\gamma}$ (given in table 2) for the corresponding E_f. The intensities i_γ are given in percent per decay. The transitions marked by the sign (a) were not placed in the decay scheme[9]).

back-shift. The radiative strength function for E1-transitions is determined[12]) from the cross-section of the (γ,n) inverse reaction. Partial widths of M1- and E2-transitions are proportional to E_γ^{2L+1}; L is the transition multipolarity.

We have also determined the widths of the E1-transitions using the model reported in ref.[13]). The necessity of using this model comes from its success not only in describing the experimental data of spherical nuclei , such as ^{137}Ba and ^{144}Nd, but also in describing[14]) the deformed nucleus ^{181}Hf. However, the results obtained from this model, in our case, did not show its success because :

- The total intensity, $I_{\gamma\gamma}$, has a weak dependence on the absolute values of radiative strength function, while it depends strongly on a function which is sensible to the energy of the transitions.
- The model[13]) does not include the local enhancements of the partial widths at some excitation energies. These enhancements were reported earlier[5]) and shown here in figure 4.

The correlations between E1-,M1- and E2- transition widths at E_γ = 6.9 MeV were taken near to the experimental values[15]) and the data of levels below 1.52 MeV and their decay modes were included in our calculation and taken from ref.[9]). Figure 3 shows that, similarly to other deformed nuclei, there may exist cascades of relatively high intensity. The probability of their random appearance is very small as shown in ref.[5]) for ^{168}Er.

5. Main peculiarities of the ^{158}Gd compound-state decay

The presence of intensified cascades contradicts the assumption that the mean width of a transition depends monotonically on the transition energy and not on the structure of the states belonging to this transition. We have shown earlier[16]) that it is not possible to describe the γ-decay cascades of compound-states in even-odd nuclei in the

4s- maximum neutron strength function region without taking into account the influence of both compound and final state structures on the partial widths of cascade transitions. It was also necessary to assume that the part of primary transitions (correlated with reduced neutron widths) in neutron resonance decay carries about one-half of their total intensity[16]).

Some correlations were found[17]) when comparison was made between the experimental distribution of maximum positions of cascade intensities and the calculated strength distribution of fragmented single quasi-particle states $K^\pi[\, N\, n_z\, \Lambda\,]$. Such calculations were made using the quasi-particle phonon model; for instance for the 1/2⁻[521], 1/2⁻[510], 1/2⁻[501] and 3/2⁻[501] states. Taking into account the fact that the above mentioned quasi-particle states contain large components of 3p neutron states the authors[17]), using the known theoretical coefficients for decomposing the wave functions on spherical basis, offered a qualitative explanation for the main local strengths of the cascades observed in the neutron resonance decay of even-odd complex nuclei in a relatively narrow excitation energy interval. The explanation is mainly based on the single-particle transitions between the 4s and 3p neutron shells. This enhancement is now being observed[16]) only in nuclei having a large enough, greater than the mean value, reduced neutron width.

The compound-states decay in even-even complex nuclei is rather difficult to interpret as a whole. However, as in even-odd nuclei, the intensity of the two-step cascades between the states having opposite parities exceeds the analogous value predicted from simple model calculation. Although figure 3 illustrates this situation clearly enough, a comparison[8]) between distributions of the experimental cascade intensities (summed over a large energy interval $\Delta E \simeq 500$ keV) and that calculated as a function of their primary transition energies gives even a better illustration of this phenomenon. Such comparison is shown in figure 4,

where the histogram represents the experimental distribution and the shaded areas correspond only to experimental statistical errors. The comparison was made here with two model calculated distributions using two different shapes of the level density dependence on the nuclei excitation energy below B_n. They are :

- the Fermi-gas model with back-shift and two free parameters [10], a and δ , where the moment of inertia is equal to one half of the rigid momentum.
- the Fermi-gas model which takes into account [11] the shell inhomogeneities of a single-particle spectrum and employs the shell corrections approach developed by Strutinsky.

In the latter case, the dependence of the level density parameter, a, on the excitation energy, U, may be expressed in the form :

$$a(U) = \hat{a}(A)\,[\,1 + f(U) * \delta E_0 / U\,]$$

with the following asymptotic expressions :

$$\hat{a}(A) = 0.048\,A + 0.257\,A^{2/3}$$

$$f(U) = 1 - \exp(-0.062\,U).$$

The numerical constants in these expressions were determined [in ref.[11]] for a wide range of mass numbers. When a value of δE_0=-0.15 MeV was used as the shell correction for ^{158}Gd, the experimental[6] value of 4.9 eV for the average spacing between resonances with J=1,2 can be deduced from our calculation. The increase of the level densities due to the presence of the vibrational states was also taken into account as recommended by the authors[11].

Although this model[11] works specially well at high excitation energies (above B_n), we have included it in our calculation because it provides good agreement with the experimental cascade intensity distributions. Such agreement may be attributed to the following reason. The intensity $i_{\gamma\gamma}$ depends mainly on the level density of the nucleus and the partial widths of cascade transitions. So in the calculation, most probably, the small values predicted by the model[11] for the level density at low excitation energies (U≤ 2 ÷ 3 MeV)

lead to the large relative values, as experimentally observed, for the secondary transitions to the low-lying states.

It should be noted that the observed intensified cascades (fig.4) with primary transition energies $2 \le E_1 \le 3$ MeV keep well in the frame of the results obtained earlier from the study of γ-decay cascades. In all the investigated nuclei, from ^{165}Dy to ^{187}W, the intensity of the cascades leading to the rotational band levels of the single quasi-particle state 1/2$^-$[510] exceeds the predicted value (by any model) by a factor of 1.5 to 2, or even more. In such a case, the enhancement of cascade intensities to these states is greater than those leading to any of the neighbouring final levels with spin difference $|J_\lambda - J_f| \le 2$ and with any other structure than 1/2$^-$[510].

The single quasi-particle states 1/2$^-$[510] for different nuclei in the region A ≃ 158 lie, according to[18], below the neutron binding energy by about 2 MeV. The reduced neutron width[6] of the ^{158}Gd compound-state from thermal neutron captures considerably exceeds the mean value. In this case, where the reduced neutron width of the compound-state considerably exceeds the mean value and the single quasi-particle states lie below the neutron binding energy, the cascade enhancements of the 4s-neutron shell can be observed[16,17], and the single quasi-particle 4s→3p transitions occure not only in the even-odd nuclei but also in the even-even ones.

It should be noted that, the enhancements of gamma-widths for the pygmy resonance was also observed[19] in the ^{160}Tb nucleus for the energy E_γ = 2.5 MeV. The authors[19] explained their results on the basis of a different from our model. Additional arguments in fovour of the better explanation of the enhancement mechanism can be possibly derived from the determanation of the cascade intensities in different neutron resonances of investigated nuclei.

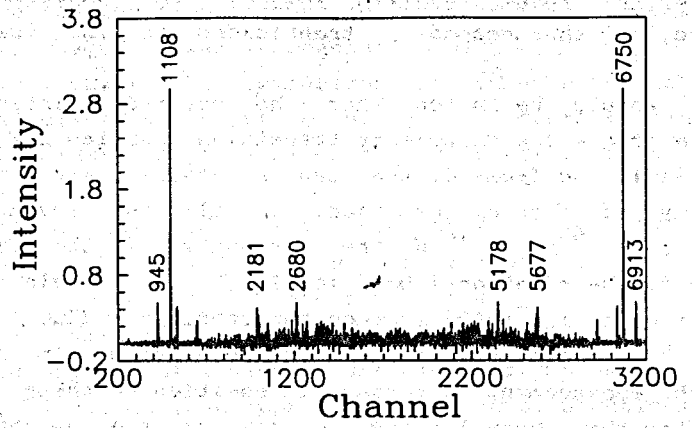

Fig. 2. The intensity, $i_{\gamma\gamma}$, distribution of two-step cascades leading to the first excited state in ^{158}Gd. Figures over peaks denote the γ-transition energies in keV. The total area of the spectrum is normalized to 100.

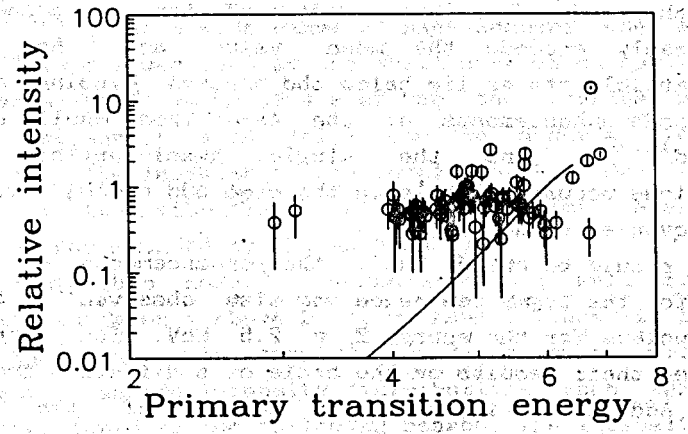

Fig. 3. Relative intensities (table 1) as a function of the primary transition energy for the resolved cascades only. Data are for the cascades which lead to the final state level at 79 keV. Line corresponds to the calculated values for the E1 + M1 cascade transitions.

6. Unresolved cascades analysis

We have determined the minimum value of the resolved cascades intensity to be $i_{\gamma\gamma}$= 0.03% per decay. This value is considered as the lower limit of our spectrometer sensitivity. For the majority of the experimentally unresolved cascades (fig.2) it is true that, the primary transitions have soft energies. But for some other unresolved cascades, the sequence of transitions is, probably, determined uncorrectly. In this case (hard primary transitions), the possible systematic-error (fig.4) can be estimated, if the number of unresolved cascades is known.

In our measurements, no other resolved transitions were observed in the two-step gamma-cascades leading to the known[9]) ten intermediate levels with spins $J^{\pi}=1^{+},2^{+}$ and 3^{+} in the energy range 1-2 MeV. If their intensities are approximately equal to our experimental sensitivity limit ($i_{\gamma\gamma}$= 0.03%), then our data (fig.4.) for the primary transitions may carry[8]), in the worst case, an error of 0.3% per decay. We may note here that an intensity of 0.8% per decay was obtained (fig.4) for this energy interval. Thus, the maximum possible systematic-error that could enter our data, (fig.4), will not exceed the value of 0.3% per decay, because it is not supposed that everyone of unobserved cascades has simultaneously an intensity of 0.03% .

On the other hand, the systematic errors caused by the transitions in the energy range 2-3 MeV, (fig.4), cannot be estimated here by a similar direct manner. Nevertheless, it must be noted that while we have had large experimental values for the cascade intensities in the analysed energy interval (fig.4), no indication of a pronounced maximum could be found in the analogous data[8]) from the decay of the ^{174}Yb compound state. The last nucleus has, (if compared with ^{158}Gd) approximately equal values for the B_n and $\langle D_\lambda \rangle$ parameters and the same parity for the compound state, and consequently we suppose that they have the same systematic errors.

The use of more efficient detectors (of efficiency two or three times higher than ours) will evidentely improve the results. In this case, for a nucleus such as ^{158}Gd, we may have a value of $I_{\gamma\gamma} \simeq 50$ % per capture, or even higher for the total intensity of observed cascades. Also the absolute systematic-error in the intensity distribution ,(fig.4), for all primary transitions (with energies $\leq$ 3 MeV) will not exceed, in such a case, some tenths of percent per capture.

7. Conclusion

In ^{158}Gd, as in other rare earth nuclei, the total intensity of observed cascades with two dipole transitions of different multipolarities (E1+M1) exceeds by a factor of 1.5 to 2 the analogous predicted value from the statistical theory. The comparison between the experimental cascades intensity distribution, fig.4, (as a function of the cascade primary transition energy) and the model calculated one has revealed the intense cascades group with primary transition energies lying in the interval 2-3 MeV. The total intensity enhancement of these cascades in this energy interval is about 15 to 20 % of the total experimental intensity summed over all the observed cascades.

In the frame of a qualitative explanation of this phenomenon, the results manifest the considerable role of the quasi-particle state transitions between the 4s and 3p shells in both even-odd[5,16,17]) and even-even complex nuclei. The maximum discrepancy between the experimental and calculated cascades intensity is found to be in the region A $\simeq$ 160. The calculated positions of the single quasi-particle neutron states $1/2^-[510]$ are in good agreement with the excitation energy of the enhanced cascade intermediate levels.

Authors thanks are due to Mrs. T.F.Drozdova for her help in the preparation of the English version of this paper.

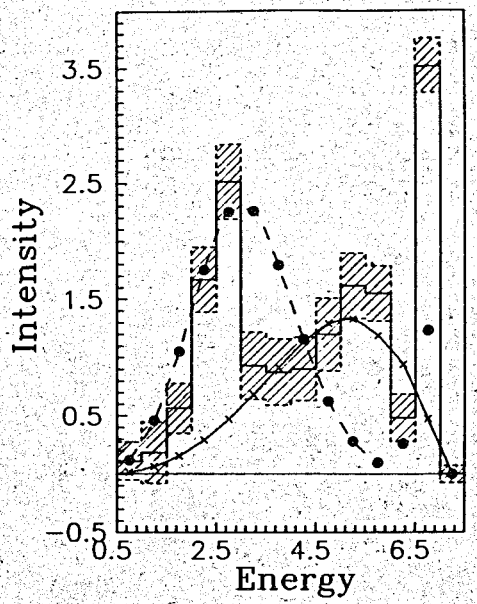

Fig.4. Cascade intensities, summed over an intermediate levels energy bin of 0.5 MeV. The cascades lead to the first three final states, and analyzed as a function of their primary transition energies per 100 decays. The histogram represents the experimental data; shaded areas are the statistical errors. (•) show the calculated values according to the level density model[11]); while x's correspond to the values predicted by the model[10]).

REFERENCES

1) A.M.Sukhovoj and V.A.Khitrov, Sov. J.: Prib. Tekhn. Eksp. 5 (1984) 27.
2) S.T.Boneva, E.V.Vasilieva and A.M.Sukhovoj, Izv. Akad. Nauk. SSSR, Ser. Fiz. 51 (1987) 1923.
3) S.T.Boneva, E.V.Vasilieva, E.P.Grigoriev, Yu.P.Popov, A.M.Sukhovoj and V.A.Khitrov, Izv. Akad. Nauk. SSSR, Ser. Fiz. 53 (1989) 884.
4) Yu.P.Popov, A.M.Sukhovoj, V.A.Khitrov and Yu.S.Yazvitsky, Yad. Fiz. 40 (1984) 573.
5) S.T.Boneva, E.V.Vasilieva, Yu.P.Popov, A.M.Sukhovoj and V.A.Khitrov, Particles and Nuclei 22 (1991) 479.
6) S.F.Mughabghab, Neutron Cross-Sections Vol.1, PartB, N.Y. Academic Press 1984.
7) Yu.P.Popov, A.M.Sukhovoj, V.A.Khitrov and Yu.S.Yazvitsky, Izv. Akad. Nauk. SSSR, Ser. Fiz. 48 (1984) 891.
8) S.T.Boneva, V.A.Khitrov, A.M.Sukhovoj and V.A.Vojnov, Z. Phys. A - Hadrons and Nuclei 338 (1991) 319.

9) R.C.Greenwood, C.W.Reich, H.A.Baader, H.R.Koch, D.Breitig O.W.B.Schult, B.Fogelberg, A.Backlin, W.Mampe, T.Von Egidy and K.Schreckenbach, Nucl. Phys. A 304 (1978) 327.
M.A.Lee, Nucl. Data Sheets 56 (1989) 199.
10) W.Dilg, W.Schutl, H.Vonach, Nucl. Phys. A 217 (1973) 269.
11) A.V.Ignatiuk, G.N.Smirenkin, A.S.Tishin, Yad. Fiz. 21 (1975) 485.
12) P.Axel, Phys. Rev. 126 (1962) 671.
13) S.G.Kadmensky, V.P.Markushev, V.I.Furman, Yad. Fiz. 37 (1983) 277.
14) A.M.Sukhovoj, Nuclear Spectroscopy and Structure of Atomic Nuclei, Leningrad, "Nauka", 1991, p.78.
15) L.M.Bollinger and G.E Thomas, Phys. Rev. C2 (1970) 1951.
16) S.T.Boneva, V.A.Khitrov, Yu.P.Popov, A.M.Sukhovoj and Yu.S.Yasvitsky, Z. Phys. A 330 (1988) 153.
17) S.T.Boneva, V.A.Khitrov, L.A.Malov, Yu.P.Popov, A.M.Sukhovoj and E.V.Vasilieva, Yamada Conf.XXIII, Nuclear Weak Process and Nuclear Structure, Ozaka, Japan, June 12-15,1989. Ed. M.Morita, World Scientific Publishing Co. Ptc.Ltd. and Yamada Science Foundation, Singapore, p.372.
18) V.G.Soloviev, Particles and Nuclei 3 (1972) 770.
19) M.Igashira, H.Kitazawa, M.Shimzu, H.Komano, N.Yamamuro, Nucl. Phys. A 457 (1986) 301.

Received by Publishing Department
on September 25, 1991.